Wavelet and Neural Network Model for Prediction of Dry Bulk Shipping Indices

Dr. Ventsislav Nikolov
Senior Software Developer
Eurorisk Systems Ltd.
31, General Kiselov Str., 9002 Varna, Bulgaria
E-mail: vnikolov at eurorisksystems dot com

Yordan Leonov
PhD student
Technical University of Varna
1, Studentska Str., Varna, Bulgaria
mcity at abv dot bg

Abstract

Shipping markets are typically volatile in nature, manifested by the dynamics of their freight rates. According to the shipowners' risk propensity, volatility related decisions vary from what kind of contract (time/voyage charter) to whether to entry/exit the business. After a sharp drop at the end of 2008, a discussion about appropriate risk management concepts and statistical tools is a need. Due to heavy investments made in the business any additional information regarding the future direction of the market volatility is of the utmost importance. The ambition of this article is exactly the same: to study fluctuations of the Baltic Panamax route 2A and the Baltic Panamax route 3A, by hybrid model of wavelets and neural networks, a new analysis tools for the shipping economics. The wavelet multiscale decomposition of time series would reveal volatility dynamics across different time frequencies and uncovered patterns will be used by neural networks for prediction.

Keywords

Dry Bulk Shipping, Wavelet, Neural Network

Wavelet and Neural Network Model for Prediction of Dry Bulk Shipping Indices

Introduction

In shipping, while planning their investment policies, agents should decide among different risk/gain ratios: how to manage risk in the light of short-term or long-term contracts in order to reduce exposure to the market highs and lows or how the portfolio of contractual agreements, either in physical market or in the paper (of shipping derivatives) to be structured. According to the shipowners' risk propensity, decisions may vary but the volatility dynamics and volatility correlations within a portfolio of assets or contracts remain a starting point[1]. However, after such events, as a sharp drop in freight levels from the end of 2008, a discussion about appropriate risk management concepts and statistical tools is a need. Due to heavy investments made in the business any additional information regarding the future direction of the market volatility is of the utmost importance.The ambition of this article is exactly the same: to study fluctuations of the Baltic Panamax route 2A and the Baltic Panamax route 3A, by hybrid model of wavelets and neural networks, a new analysis tools for the shipping economics. Following this introduction, we devote Section 2 to the relationship of the paper with existing literature, next sections address the advantages afforded by wavelets and neural networks. The paper continues with the examination of the proposed technique and the last two sections conclude the article with the investigation of the results and proposal for further developments, based on the novelty of the method.

[1] Note should be inserted, having in mind the amount of critical voices towards using David X. Li's Gaussian copula (which defines the relationship between two assets/variables), claiming that it never be captured by a single scalar quantity, for example in Salmon F. "Recipe for Disaster: The Formula That Killed Wall Street." Wired magazine 02/23/2009

Volatility. Models

In shipping economics literature, Kavussanos(1996a) examines freight rates and ship price volatilities, making comparison over different ship sizes. His findings acknowledge that smaller class vessels, due to their commercial flexibility, attract less volatility compared to bigger classes. The other pattern found is "*…clear tendency for volatility clustering…*" over individual dry shipping markets. This feature, as firstly suggested in (Mandelbrot, 1963), means that "*large changes tend to be followed by large changes, of either sign, and small changes tend to be followed by small changes*". Consequently, returns are not independent across time and on the other hand there is nolinear autocorrelation. The latter suggests those series are heteroskedastic, and are preferably modeled by most used variant of the autoregressive conditional heteroskedastic models: called GARCH, after generalized ARCH (Bollerslev, T., 1986). In (Kavussanos, M., 1996), GARCH models are used to present volatility in shipping markets, as a time varying process. Fractionally Integrated GARCH (FIGARCH) model, as a long-memory model for absolute returns can be found in (Nomikos et al., 2009), it is pointed out as alternative to GARCH in specification of volatility dynamics of weekly spot freight rates for the dry Capesize market, as well for VLCC, Suezmax and Aframax tanker markets. Critics about the GARCH models as conventional parametric methods can be found in (Taleb, 2007), who advocate that stochastic volatility and GARCH/Extreme Value Theory are approaches that do not solve the problem of confidence about small probability of events that are not in the sample of the past realizations. Volatility swings, as those in dry freight bulk market, ARCH/GARCH methodology try to explain, as in (Greene, W. H., 2002: 238), like "*…model errors, which appear in clusters…*". This problem, as (Ramsey, J. B., 1999) asserts, can be tackled by wavelets, with approximation of long memory processes, without knowledge of their underlying function. (Gencay, R. et al., 2001) have argued that wavelets can decorrelate non-stationary time series, like financial ones, where market participants' interactions occur at different time scales. Different specifications of GARCH models are investigated in shipping: threshold GARCH (TGARCH) and exponential GARCH (EGARH) in (Alizadeh Amir H., 2009) try to reveal possible asymmetric impact of positive and negative shocks of volatility of VLCC TD3 and Capesize C4 spot rates. The review of the above models can be found in authors' words in pp 92-93 "*…three estimated volatilies for VLCC*

TD3 and Capesize C4 are very close, with minor differences due to the structure of the models…". As in each of the time-varying variance approaches, fully examined in (Alizadeh Amir H., 2009: pp. 80-106), we produce univariate forecast of future volatility by a hybrid approach. In order to align our results with the benchmark model, we compare it to GARCH (1,1)[2].

The multi-resolution analysis. The pyramid algorithm. The discrete wavelet transformation.

The idea of multi-resolution analysis, used in the paper, is to present time-series as sum of smooth and detail coefficients. If the initial signal is $x(t) \in L^2$ and an initial resolution is *J*, the presentation in (Daubechies, I., 1982) (Mallat, S. G., 1999) follows in (1):

$$x(t) = \sum_{n \in Z} c_{J,n} \phi_{J,n}(t) + \sum_{j=J}^{\infty} \sum_{n \in Z} d_{j,n} \psi_{J,n}(t) \quad (1)$$

where $\psi(t)$ and $\varphi(t)$ denote respectively the wavelet and the scaling function. The details coefficients $d_{j,n}$ are presented in (2) and the scaling coefficients $c_{j,n}$ are defined in (3):

$$d_{j,n} = 2^{-\frac{j}{2}} \int_{-\infty}^{+\infty} x(t) \psi_{j,n}\left(2^{-j} t - n\right) dt \quad (2)$$

$$c_{j,n} = 2^{-\frac{j}{2}} \int_{-\infty}^{+\infty} x(t) \psi_{j,n}\left(2^{-j} t - n\right) dt \quad (3)$$

From the output of the corresponding filters at resolution *j*, based on (2) and (3), the coefficients at finer level of resolution $(j-1)$ of a scaling filter g_l (4) and the coefficients of a wavelet filter h_l (5) are generated by downsampling by a factor of two. The computation, in the opposite direction, of coefficients from those at the coarser level of resolution is according to (6).

[2] For addressing GARCH properties, one can consult Alizadeh and Nomikos (2009) pp.103-105

$$c_{j,n} = \sum_{l \in Z} g_l c_{j-1,2n-l} \tag{4}$$

$$d_{j,n} = \sum_{l \in Z} h_l c_{j-1,2n-l} \tag{5}$$

$$c_{j-1,n} = \sum_{l \in Z} g_l c_{j,2n-l} + \sum_{l \in Z} h_l d_{j,2n-l} \tag{6}$$

The equations (4) - (6) reveal a pyramid algorithm (Mallat, S. G., 1999) or discrete wavelet transform (DWT). The DWT suffers from some limitations (Percival, D. B., A. T. Walden, 2000):

1) it is not a time (shift)-invariant transform: shifting $x(t)$ by some amount does not ensure that the corresponding wavelet and scale coefficients are translated by the same amount;
2) dyadic length requirements, induced by the downsampling when computing the transform.

In response to that, the maximum overlap discrete wavelet transform (MODWT), also known as the “non-decimated wavelet transform” or the “stationary DWT” or the “translation invariant DWT” has been developed. A thorough discussion of it could be found in (Gencay, R. et al., 2001) (Percival, D. B., A. T. Walden, 2000).

As mentioned, MODWT gives up the downsampling (decimation) at each scale[3]. Contrary to the DWT, in MODWT, down-sampling of the signal is changed with up-sampling at each level of decomposition, which makes MODWT shift-invariant and as clearly described in (Crowley, P., 2005: 32) ”*…In contrast to the DWT the MODWT simply skips the downsampling after filtering the data, and everything else described in the section on MRDs using DWTs above follows through, including the energy (variance) preserving property and the ability to reconstruct the data using MRA with an inverse MODWT…*”

[3] However, for time series of dyadic length, it may be subsampled and rescaled to obtain an orthonormal DWT.

The Maximal Overlap Discrete Wavelet Transform

As in (Percival, D. B., A. T. Walden, 2000), the wavelet filter must satisfy the following properties:

$$\sum_{l=0}^{L-1} \tilde{h}_l = 0 \tag{7}$$

$$\sum_{l=0}^{L-1} \tilde{h}_l^2 = \frac{1}{2} \text{ and } \sum_{L=-\infty}^{\infty} \tilde{h}_l \tilde{h}_{l+2r} = 0 \tag{8}$$

The scaling filter $\{\tilde{g}l\}$ must answer conditions (9), where L denotes the length of the wavelet filter

$$\sum_{L=0}^{L-1} \tilde{g}l = 1 \tag{9}$$

Intuitively, (7) means that the average value of the wavelet in the time domain must be zero and therefore it must be oscillatory.

The MODWT pyramid algorithm, where the wavelet coefficients $\{d_{j,n}^{(M)}\}$ and the scaling coefficients $\{c_{j,n}^{(M)}\}$ are generated, using the filters $\{\tilde{h}_{j,l} = h_{j,l/2^{j/2}}\}$ and $\{\tilde{g}_{j,l} = h_{j,l/2^{j/2}}\}$ is presented in (10):

$$d_{j,n}^{(M)} = \sum_{l=0}^{Lj-1} \tilde{h}_{j,l} x_{n-l \bmod N}$$

$$c_{j,n}^{(M)} = \sum_{l=0}^{Lj-1} \tilde{g}_{j,l} x_{n-l \bmod N} \tag{10}$$

In (10) M stands for MODWT and N denotes the length of the time series to be analyzed. Using the inverse pyramid algorithm proposed in (Percival, D. B., A. T. Walden, 2000), the original time series can be recovered from (11):

$$c_{j-1,n}^{(M)} = \sum_{l=0}^{L-1} \tilde{h}_l d_{j,n+2^{j-1}l \bmod N}^{(M)} + \sum_{L=0}^{L-1} \tilde{g}_l c_{j,n+2^{j-1}l \bmod N}^{(M)} \quad (11)$$

Figure 1.x: Maximal Overlap Discrete Wavelet Transform

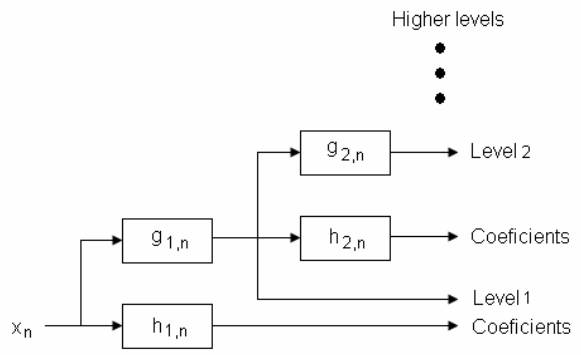

Neural network processing

First, the initial time series is decomposed in different wavelet time frequencies, then every frequency is predicted as an independent time series and finally the predicted time frequencies are composed in order to obtain the final predicted time series – Fig.1. The mathematical model of the neural network is an adjustable structure that works in two main stages (Fausett, L., 1994) (Tang, Z., P. A. Fishwick, 1993) (Fig. 2).

Figure 2.: Wavelet decomposition of the initial time series, prediction of the separate sequences and reverse composition to the series with predicted values

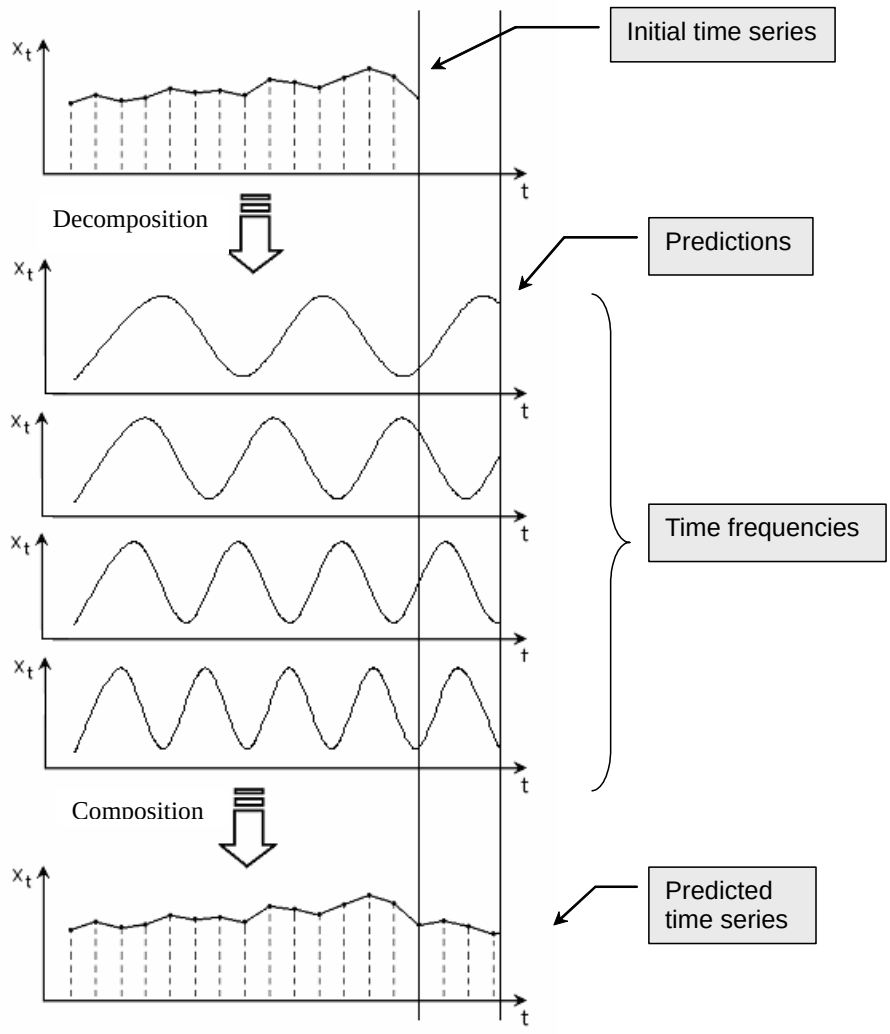

Figure 3.: Neural network training and prediction

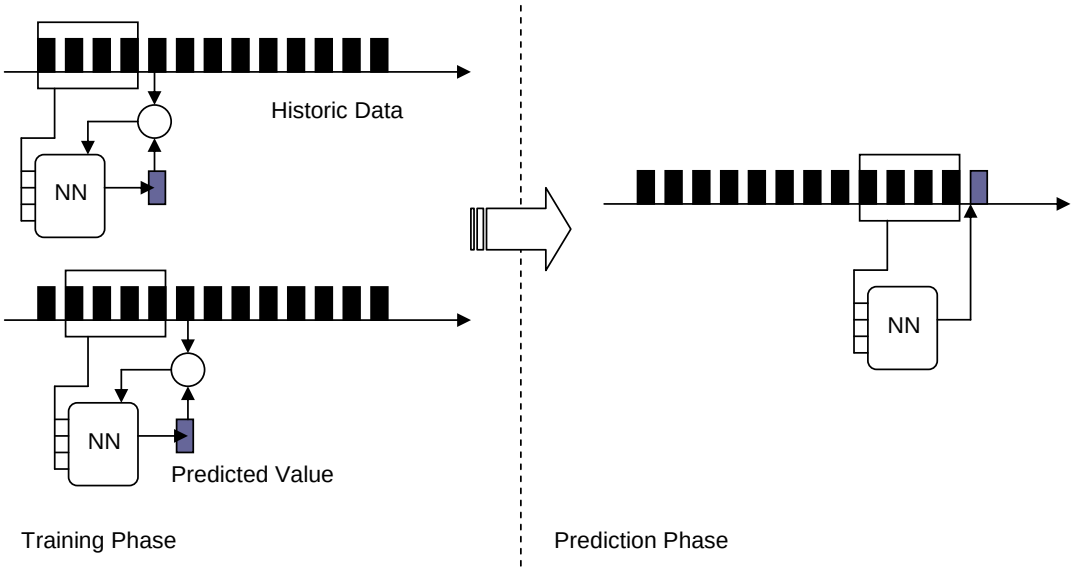

1) Training using the available historical data. Here the training examples are collected by usage of "*sliding time window*" (Zhang, G. P., 2004). The size of the window is usually estimated by different heuristic methods. Here the autocorrelation function is analyzed for this purpose (Chatfield, C., 1996).
2) Prediction in a given time horizon. When the training completed the neural network is fed by the last values and it generates a prediction. In this sense the neural network works as a function that generate a prediction based on the previous known values:

$$x(t+1) = f\left[x(t), x(t-1), x(t-2), \ldots, x(t-n)\right] \quad (12)$$

Further a recursive prediction is applied until the desired horizon is reached.

Every time frequency is considered as a time series that is individually pre-processed (forward processing), predicted by a multilayer perceptron, and post-processed (backward processing).The used technique of recursive prediction requires preliminary transformation of the data in order to be within the neural network activation function. This means that every predicted value is considered as a real one and used as a neural network input. The output predicted value is in the range of the activation function and therefore all input values must also be transformed to be into this range. The most commonly used activation function in the multilayer perceptrons is in the range of $[0,1]$ or $[-1,1]$.

The problem of this transformation is eventual mismatch between the predicted and the training data. Let the whole time series before applying of the sliding window approach consists of *n* values (data used for training) and prediction is needed when the series length is $n+k$ (current data) and the last k of them contains a minimum or maximum that is below respectively above the minimum/maximum of the first n values. This situation is illustrated in Fig. 3, where the maximum value of the current data is different than this of the training data. If the training data is in the range $[\min, \max]$ and it is transformed into $[-1,1]$, after obtaining the next k values, the new range $[\min, new\max]$ will be transformed into $[-1,1]$, which means that the first n values will be transformed into unrecognizable for the neural network data, although they have been in the training set.

To overcome the problem, the data transformation is parametrized, where the starting point is the equation (13) , used for the ordinary data scaling:

$$y = min + (x - smin)\frac{max - min}{s\,max - s\,min} \tag{13}$$

where y is the transformed value; $\min$ and $\max$ are minimum and maximum values of the new range; $s\min$ and $s\max$ are minimum and maximum of the initial data values; x is the current value of the initial time series. These calculations may also be done as the following two steps:

1) Scaling – transformation of the original data to be in the range of the activation function range;
2) Shifting – the time series is shifted to be centered about *Y* axis.

These steps can be done using parameters ξ and ψ , which define the scaling and shifting respectively:

$$\xi = \frac{max - min}{s\,max - s\,min} \tag{14}$$

$$\psi = min - s\,min \cdot \xi \tag{15}$$

After performing these two steps the parameters ξ and ψ should not be changed any more. Thus, when they are already calculated, adding or removing values to/from the time series does not change the training data range. Using these parameters, the forward transformation is as follows:

$$y = x\xi + \psi \tag{16}$$

and the backward transformation is:

$$x = \frac{y - \psi}{\xi} \tag{17}$$

Figure 4.: The turning up new data values makes the time series to be in a different range compared to the training data

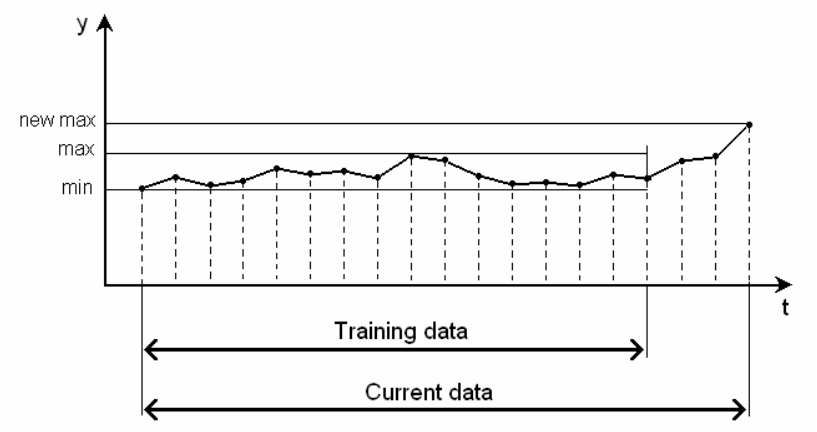

The information about the transformations applied to the time series should be kept together with the parameters ξ and ψ, which should also be used for the backward transformations to restore the range of the predicted values generated by the neural network using formula (5). Moreover, in order to minimize the probability the new k values to be out of the activation function range, the scaling is usually performed in $[-0.9,0.9]$ instead of $[-1,1]$.

Sequence of transformations on time series

The pre-processing of the data is done before the neural network training and prediction. After obtaining the predicted values backward transformations should be done. All transformations could be divided into groups according to their type:

1) Transformations to make stationary time series;
2) Scaling and translation;

Note that the scaling of the time series within the range $[0,1]$ or $[-1,1]$ could be done in different ways. For example, transformation of the original data within $[0,1]$ when $\min(x_t) = 0$ and $\max(x_t) = 1$ may change the autocorrelations. However, if the scaling is done by dividing each time series value x_t by $\max(x_t)$, the values will also be in the range $[0,1]$, but if $\min(x_t) \neq 0$, then $\min(y_t) \neq 0$. In this case the whole range $[0,1]$

will not be used but the autocorrelations will be preserved. As it is known the autocorrelation is calculated as follows:

$$r_k = \frac{\sum_{t=1}^{n-k}(x_t - \bar{x})(x_{t+k} - \bar{x})}{\sum_{t-1}^{n}(x_t - \bar{x})^2} \tag{18}$$

After dividing x_t by $\max(x_t)$ the following result is obtained:

$$r_k = \frac{\sum_{t=1}^{n-k}\left(\frac{x_t}{max(x_t)} - \frac{\bar{x}}{max(x_t)}\right)\left(\frac{x_{t+k}}{max(x_t)} - \frac{\bar{x}}{max(x_t)}\right)}{\sum_{t-1}^{n}\left(\frac{x_t}{max(x_t)} - \frac{\bar{x}}{max(x_t)}\right)^2} = \frac{\left(\frac{1}{max(x_t)}\right)^2\sum_{t=1}^{n-k}(x_t - \bar{x})(x_{t+k} - \bar{x})}{\left(\frac{1}{max(x_t)}\right)^2\sum_{t-1}^{n}(x_t - \bar{x})^2} = \frac{\sum_{t=1}^{n-k}(x_t - \bar{x})(x_{t+k} - \bar{x})}{\sum_{t-1}^{n}(x_t - \bar{x})^2} \tag{19}$$

The result is the same as in equation (18). As the sliding window size is estimated by analyzing sample autocorrelation function, the pre-processing of the initial time series should be precisely considered.

Figure 5.x: Maximal Overlap Discrete Wavelet Transform and Prediction

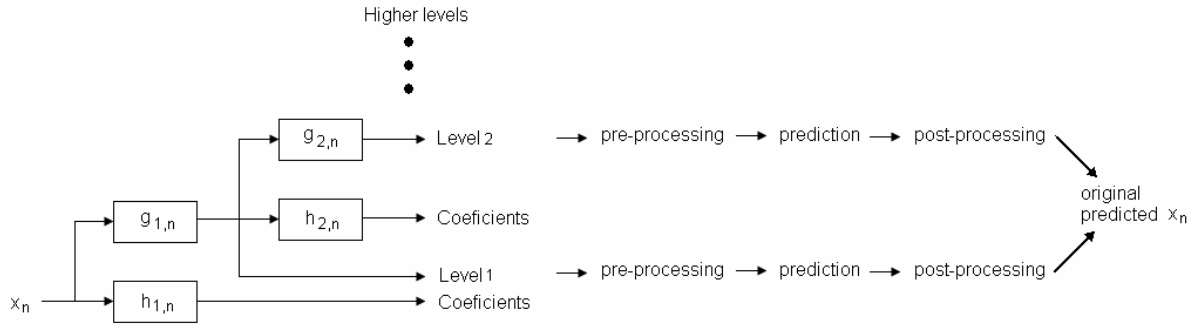

Implementation and Results

To provide an example of wavelet decomposition, we consider P2A[4] and P3A daily volatility series. The volatility v_t is measured by the absolute returns, $v_t = |r_t|$, where $r_t = \log(p_t) - \log(p_{t-1})$ is the first difference of log-transformed daily index values. From the plotted figures we see for both of the series, that exhibit low volatility behavior up to observations 2230 in P2A case and 2350 in the P3A plot. Since with MODWT, we are not limited to the dyadic sample size, we use all available data, respectively vectors of length of 2713, 2676 units. Having in mind the requirement that the depth of transform must answer to $J \leq \log_2(N)$, where N is sample size, we choose to perform at $J = 5$ (levels of decomposition meaning we are able to capture frequencies up to 2^5 = 32 days, near to the time charter contract periods (see the data table). The analysis uses the Haar wavelet, appropriate for describing of non-stationary samples, as those at the end of investigated series, when volatility bumped. Dealing with undesirable boundary effects, we use the so called circular shifting (the shifting of data from an end of series to the start, in order to execute approximations). The wavelet scale (smooth) coefficients for both of the series, corresponding to low-frequency trends, obviously capture significant increase in volatility, around zones 2230-2450 (P2A) and 2350-2640 (P3A). On the other hand details at levels 3 to 5 (Fig. 4(c-e)) and details coefficients in Fig. 5(c-d), are quite descriptive themselves about volatility oscillations, suggesting that the trading horizon is around a month (recognizable cycles for frequency from 2^4 = 16 to 32 days) for the Trans-Pacific round voyage (P3A) and within 32-64 days, allowing sufficient time for the market information to reflects the future freight levels. This is partly expected, as time-charters thought to be average of expected spot rates over the duration of the contracts. Comparing levels 3 for both routes (Fig.4e and Fig.5e) seems to confirm the assertion that the longer the duration of the contract, the smoother the rates, presented here by absence in P2A of such apparent fluctuations as in P3A (the shorter contract).

[4] The raw data is provided to us by Freight Investor Services (UK), see Table 1

The volatility swing, started in mid 2008, is clearly presented over all levels of decompositions. The results show that the wavelet neural network approach better capture the movement directions compared to the GARCH(1,1), as the comparison uses the default GARCH(1,1) model for prediction of the conditional standard deviations of the return series the particulars are shown in tables 2 and 3 show particulars of model parameters.

On Fig. 6 – 7 for five-step-ahead prediction, WNN results move similarly to the real data, where the GARCH(1,1) method produces results near to a linear trend, documented by the root mean squared error values statistics, as well.

Figure 6.: Wavelet decomposition of daily absolute returns of the P2A, presented as follows (a) original volatility series (b) scale coefficients (c)-(g) wavelet coefficients (details) of levels from 5 to 1, from top downward

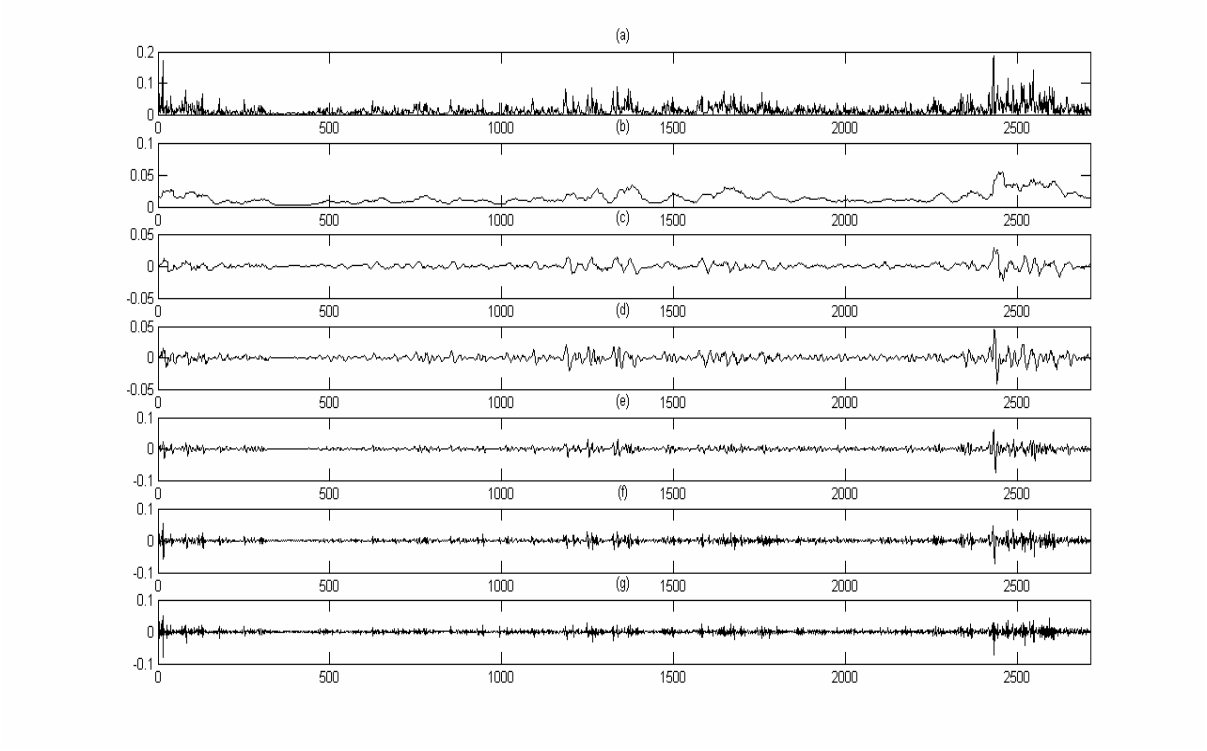

Figure 7.: Wavelet decomposition of daily absolute returns of the P2A, presented as follows (a) original volatility series (b) scale coefficients (c)-(g) wavelet coefficients (details) of levels from 5 to 1, from top downward

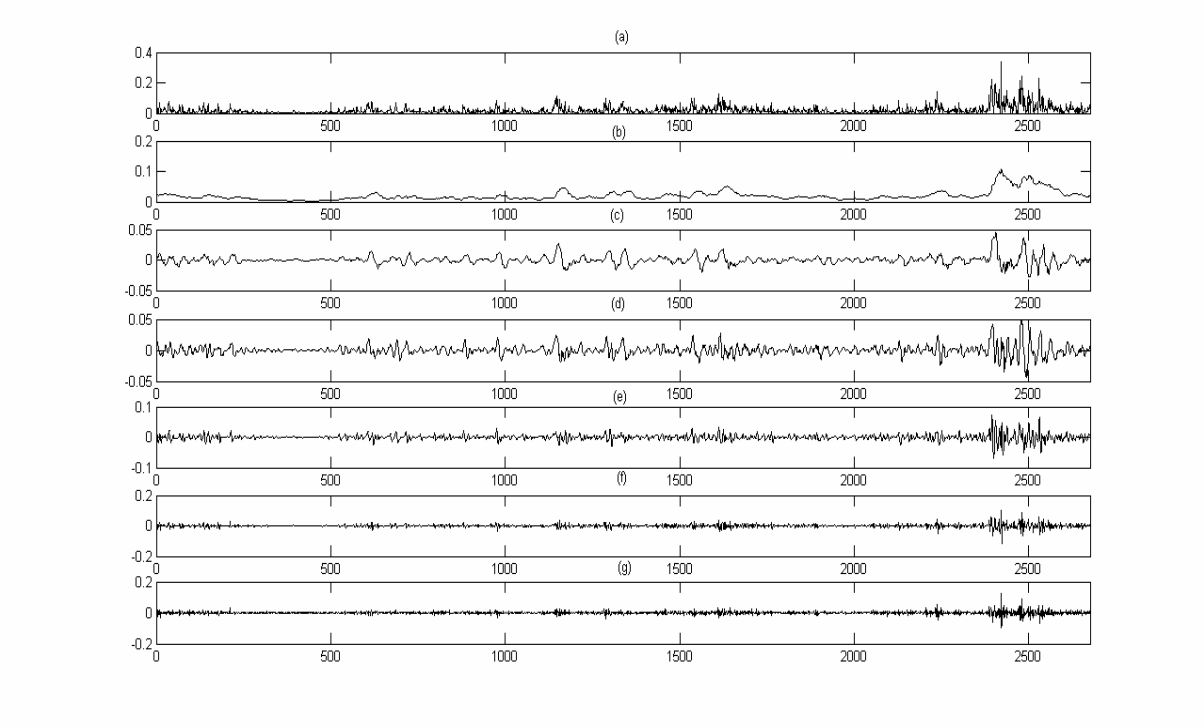

Figure 8.: A Comparison of forecasting performance for five-step-ahead predictions generated by the WNN and GARCH(1,1) models for the Panamax Route 2A

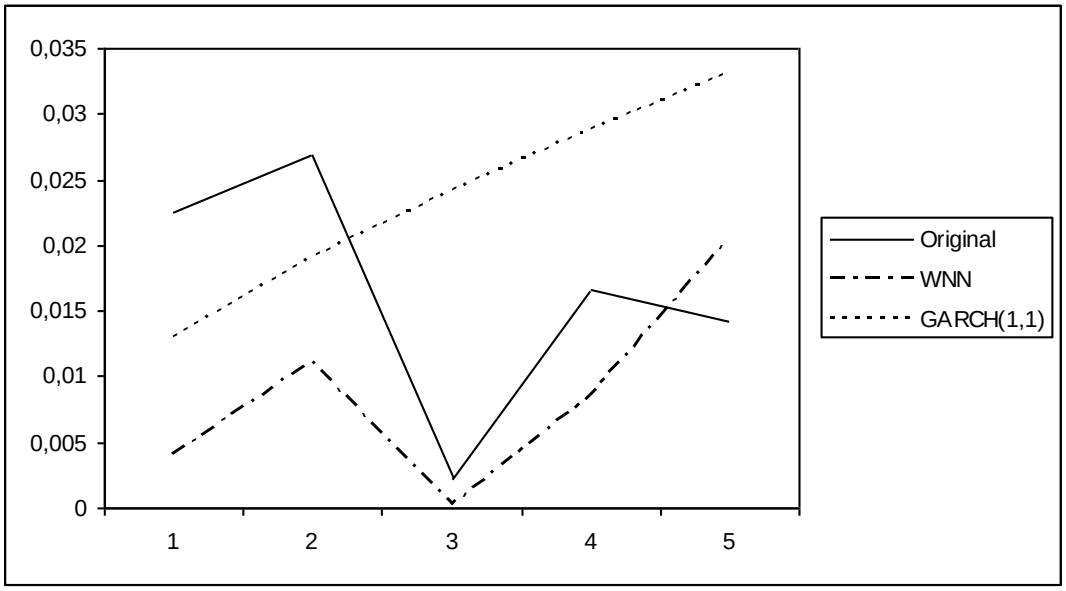

Root mean squared error:

- wavelet neural network method – 0,011862564
- GARCH method – 0,015076109

Figure 9.: A Comparison of forecasting performance for five-step-ahead predictions generated by the WNN and GARCH(1,1) models for the Panamax Route 3A

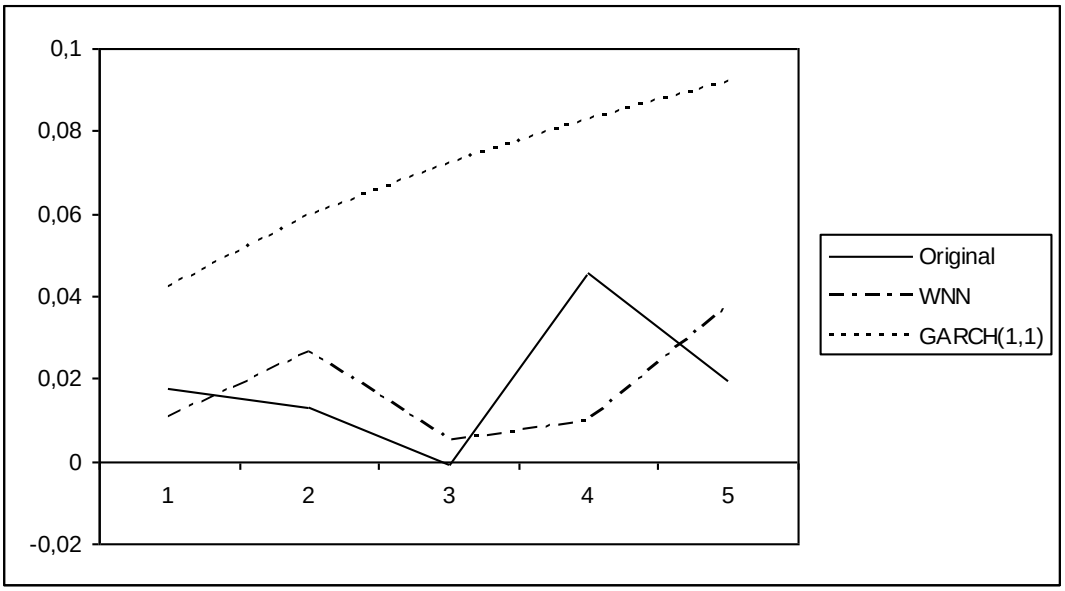

Root mean squared error:

- wavelet neural network method – 0,019519453
- GARCH method – 0,054190628

Conclusion

In this paper we have presented the theoretical framework of design of wavelet neural network model, which reveals good approximation of predicted volatility series. The success of the proposed algorithm resides on the wavelet ability to decompose original series to trend and local behaved series which serve as activation functions in neural network, learning algorithm. The local adaptiveness of wavelets allows them to study non-stationarities, like sudden ruptures and clusters. It gives useful insight into volatility dynamics. The wavelet multi-resolution analysis can motivate investigation of relationship between volatilities in different scales, related to the rate of flow of information amongst players with different investment horizons. If applied to implied volatility of derivative contracts, the proposed algorithm could be used as a tool in spot price discovery.

References

1. Alizadeh Amir H. and Nomikos Nikos K. Shipping derivatives and risk management in shipping. Palgrave Macmillan, 2009.
2. Bollerslev, T. Generalised autoregressive conditional heteroskedastic. Journal of Econometrics, vol.31, 1986, pp. 307 – 327.
3. Brockwell, P. J., R. A. Davis. Introduction to Time Series and Forecasting, second edition. Springer, 2002, p. 434.
4. Chatfield, C. The analisys of time series. An introduction. Fifth edition. Chapman & Hall/CRC, ISBN-10: 0412716402, ISBN-13: 978-0412716409, 1996, p. 304.
5. Crowley, P. An intuitive guide to wavelets for economists Bank of Finland Research Discussion Papers 1, 2005.
6. Daubechies, I. Ten Lectures on Wavelets. Philadelphia, Pa, USA: SIAM, 1992.
7. Engle, R. F. Autoregressive Conditional Heteroskedasticity with Estimates of the Variance of UK Inflation. Econometrica 50, 1982, pp. 987 – 1008.
8. Fausett, L. Fundamentals of Neural Networks: Architectures, Algorithms, and Applications. Prentice-Hall, ISBN:0-13-334186-0, 1994, p. 461.
9. Gencay, R. et al. An Introduction to Wavelets and Other Filtering Methods in Finance and Economics. Academic Press, San Diego, CA, USA, 2001.
10. Greene, W. H. Econometric Analysis (5th ed.), Prentice-Hall, Englewood Cliffs, NJ, 2002.
11. Kavussanos, M. Comparison of volatility in the dry-cargo ship-sector, Journal of Transport Economics and Policy 30, 1996, pp. 67–82.
12. Kavussanos, M. Price risk modelling of different size vessels in the tanker industry, Logistics and Transportation Review 32, 1996, pp. 161 – 176.
13. Mallat, S. G. Theory for multiresolution signal decomposition: the wavelet representation. IEEE Transactions on Pattern Analysis and Machine Intelligence. 11(7), 1999, pp. 674 – 693.
14. Mandelbrot. The variation of certain speculative prices, Journal of Business, XXXVI, 1963, pp. 392 – 417.
15. Nomikos et al. An Investigation into the Correct Specification for Volatility in the Shipping Freight Rate Markets. Presentation for IAME Conference, held in Copenhagen, 2009.
16. Percival, D. B., A. T. Walden. Wavelet Methods for Time Series Analysis, Cambridge, Cambridge University Press, Chapter 5, 2000.

17. Ramsey, J. B. The contribution of wavelets to the analysis of economic and financial data. Philosophical Transactions of the Royal Society 357(1760), 1999, pp. 2593 – 2602.
18. Taleb, N. N. Black Swans and the Domains of Statistics. The American Statistician, Vol. 61, No. 3, 2007.
19. Tang, Z., P. A. Fishwick. Feed-forward Neural Nets as Models for Time Series Forecasting. ORSA Journal on Computing Vol. 5, No. 4, Fall 1993, pp. 374 – 385.
20. Zhang, G. P. Neural Networks in Business Forecasting. Idea Group Publishing, ISBN: 1591401771, 2004, p. 296.

Appendix

Table 1: Baltic Exchange Information Services Ltd/ The Baltic P2A and P3a routes

Sector	Route	Size (MT)	Price Quotation	Data period, presented in the survey
P2A **Panamax Route 2A,**	Basis delivery Skaw/Gibraltar Far East, re-delivery Taiwan/Japan range, 60/65 days. Loading 15-20 days ahead in the loading area3.75 per cent total commission	Baltic panamax 74,000 mt dwt not over 7 years, max LOA 225, draft 13.95, 14.0 knots. Cargo basis grain, ore, coal, or similar	USD/Day	31/12/1998 To 12/11/2009 2715 data points
P3A **Panamax Route 3A**	Transpacific round of 35/50 days either via Australia or Pacific; re-delivery Japan-South Korea range,	Baltic panamax 74,000 mt dwt not over 7 years, max LOA 225, draft 13.95	USD/Day	25/2/1999 To 12/11/2009 2678 data points

Table 2: GARCH(1,1) model specification for P2A route

Parameter	Value	Error	Statistic
C	0.00079652	0.0029442	0.2705
K	2.3539e-006	2.4971e-005	0.0943
GARCH(1)	0.99465	0.056268	17.6771
ARCH(1)	0.0053464	0.016822	0.3178

Table 3: GARCH(1,1) model specification for P3A route

Parameter	Value	Error	Statistic
C	0.00080065	0.0033544	0.2387
K	0.00012231	0.00012564	0.9735
GARCH(1)	0.78751	0.16898	4.6603
ARCH(1)	0.11998	0.090226	1.3297